On the Limitations of Hyperbola Fitting for Estimating the Radius of Cylindrical Targets in Non-Destructive Testing and Utility Detection

Iraklis Giannakis, Feng Zhou, Craig Warren, and Antonios Giannopoulos

***Abstract*—Hyperbola fitting is a mainstream interpretation technique used in ground penetrating radar (GPR) due to its simplicity and relatively low computational requirements. Conventional hyperbola fitting is based on the assumption that the investigated medium is a homogeneous half-space, and that the target is an ideal reflector with zero radius. However, the zero-radius assumption can be easily removed by formulating the problem in a more generalized way that considers targets with arbitrary size. Such approaches were recently investigated in the literature, suggesting that hyperbola fitting can be used not only for estimating the velocity of the medium, but also for estimating the radius of subsurface cylinders, a very challenging problem with no conclusive solution to this day. In this paper, through a series of synthetic and laboratory experiments, we demonstrate that for practical GPR survey, hyperbola fitting is not suitable for simultaneously estimating both the velocity of the medium and the size of the target, due to its inherent non-uniqueness, making the results unreliable and sensitive to noise.**

***Index Terms*—Ground-penetrating radar, GPR, non-destructive testing, utility detection, concrete, hyperbola fitting, radius estimation, utility detection, rebars.**

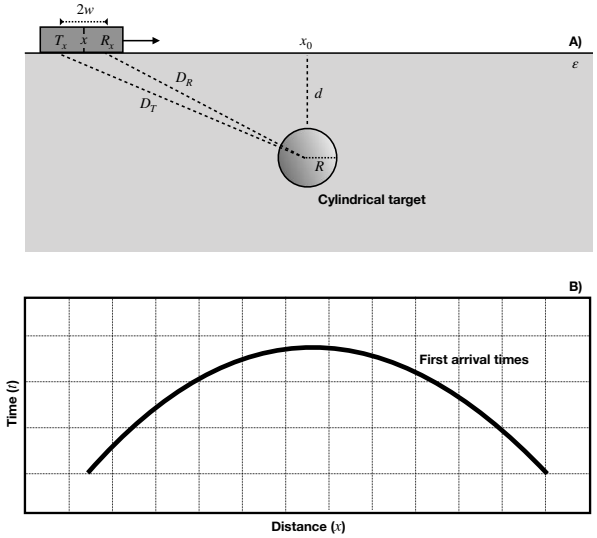

Fig. 1. A) The generic scenario under consideration in hyperbola fitting. B) The characteristic hyperbolic arrival times of cylindrical targets.

I. Introduction

GROUND Penetrating Radar (GPR) has been extensively used in various fields, from non-destructive testing and landmine detection to glaciology and environmental science [1]. Two of the most mainstream applications of GPR are utility detection and concrete inspection [2]. These applications, although different in many ways, they share the same objective, which is to detect cylindrical targets in relatively homogeneous half-spaces [3], [4].

To that extent, for both rebar and utility detection, similar signal processing approaches have been suggested over the years to remove the antenna cross-coupling, increase the overall signal to clutter ratio, and ultimately enhance the reflected signal from the subsurface cylindrical targets [5]. Apart from processing, various interpretation methods have also been suggested, from conventional radar approaches [6] to full-waveform inversion [7] and machine learning [4]. One of the most frequently used interpretation approaches in GPR is hyperbola fitting, a simple and elegant method that utilises the characteristic hyperbolic signatures of cylinders to infer their depth and size [8]–[12], and the bulk velocity of the host medium [1].

Different methods have been suggested for implementing hyperbola fitting [13]. Graphical representations via trial and error are extensively used in commercial GPR processing softwares [13]. More advanced methods like Hough transform [14] and probabilistic fitting [15] have also been successfully applied; and recently machine learning has been used for automatically detecting and characterizing hyperbolas in processed radargrams [16], [17]. All of these methods are based on the same assumptions that the measurements are taken perpendicular to a cylindrical target buried in a homogeneous half-space. Most importantly, all hyperbola fitting methodologies, utilise only the shape formed by the individual arrival times of the target reflections, without taking amplitudes into account. As a result, conventional hyperbola fitting cannot be used for estimating the dielectric properties of the targets [13]. In this paper we argue that, for the level of accuracy needed for practical engineering applications such as utility detection and concrete inspection, and in the absence of any *a priory*

I. Giannakis is with the School of Geosciences, University of Aberdeen, Meston Building, Kings College, Aberdeen, AB24 3FX, UK. E-mail: iraklis.giannakis@abdn.ac.uk

F. Zhou is with the China University of Geosciences (Wuhan), School of Mechanical Engineering and Electronic Information, Wuhan, China, 388 Lumo Rd, 430074. E-mail: zhoufeng@cug.edu.cn

C. Warren is with the Department of Mechanical and Construction Engineering, Northumbria University, Newcastle, NE1 8ST, UK. E-mail: craig.warren@northumbria.ac.uk

A. Giannopoulos is with the School of Engineering, The University of Edinburgh, Edinburgh, EH9 3FG, UK. E-mail: a.giannopoulos@ed.ac.uk

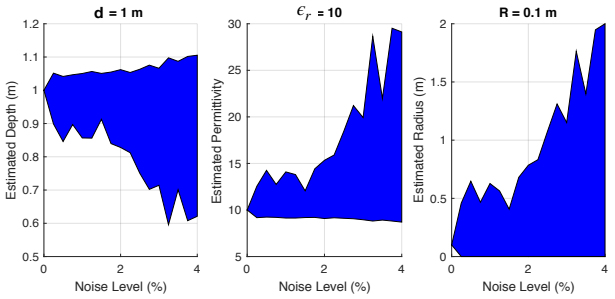

Fig. 2. Utility detection: hyperbola fitting (4) for different levels of Gaussian noise. 120 realisations of the optimization in (4) are executed for each level of noise. The real $\{d, R, \epsilon_r\}$ are shown on the titles of the subplots. With blue colour is the range of $\{d, R, \epsilon_r\}$ that equally fits the noisy data. It is apparent, than even just 2% error can result to up to 500% error on radius estimation, falsely estimating the radius of the pipe anywhere from 0 up to 0.6 m. This range includes the whole spectrum of utility sizes, adding no additional information to what is already expected.

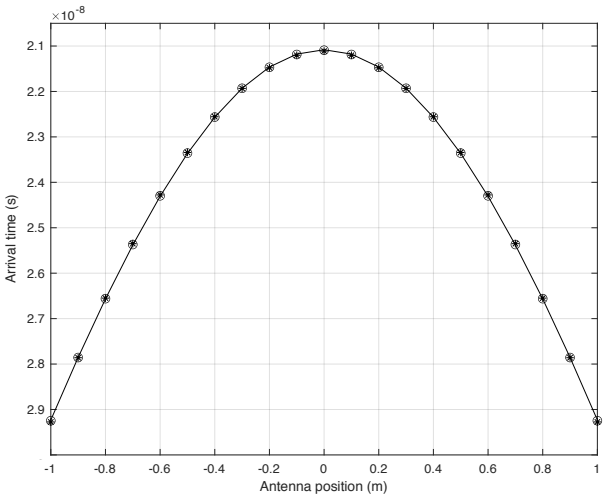

Fig. 3. Three almost identical hyperbolas with different $\{d, R, \epsilon\}$ are plotted together to illustrate the non-unique results of hyperbola fitting in the presence of noise. Solid line: $d = 1$ m, $R = 0.1$ m, $\epsilon_r = 10$; circles: $d = 0.97$ m, $R = 0.2$ m, $\epsilon_r = 10.6$; stars: $d = 0.91$ m, $R = 0.4$ m, $\epsilon_r = 12.1$.

knowledge of the medium's velocity, hyperbola fitting cannot be used for estimating the radii of cylindrical targets neither.

II. Hyperbola Fitting

Conventional hyperbola fitting assumes that ground-coupled GPR antennas move along the x-axis perpendicular to the main axis of a cylindrical target buried in a non-magnetic half-space with uniform permittivity distribution (Fig. 1). Although hyperbola fitting can be modified to address non-flat surfaces [18] and air-coupled antennas [19], nonetheless, the scenario mentioned above is the most typical and mainstream case study under consideration. Hyperbola fitting only utilises the shape of the hyperbola, meaning that it is amplitude-agnostic. Therefore, it is affected neither by the conductivity of the medium nor the permittivity of the cylindrical target. Consequently, hyperbola fitting cannot be be used to infer any of those properties.

From Fig. 1, through some elementary geometry it can be derived that, for small offset w, the two-way arrival time t (s) of the target's response is given by

$$t = \frac{(D_T + D_R) - 2R}{c_0}\sqrt{\epsilon_r} \tag{1}$$

where $c_0 \approx 2.99 \cdot 10^8$ (m/s) is the velocity of light in free space, R is the radius (m) of the cylindrical target, ϵ_r is the relative permittivity of the homogeneous non-magnetic half-space, and D_T and D_R are the distances (m) from the center of the target to the transmitter and the receiver, respectively. It is easy to show using Pythagoras theorem that

$$D_T = \sqrt{(x + w - x_0)^2 + (d + R)^2} \tag{2}$$

$$D_R = \sqrt{(x - w - x_0)^2 + (d + R)^2} \tag{3}$$

where x is the position of the mid-point of the GPR transmitting and receiving antennas (m), x_0 is the projection of the center of the target to the x-axis (m), $2w$ is the distance (m) between the transmitter and the receiver, and d is the cover depth (m) of the cylindrical target.

The first step in hyperbola fitting is to pick the arrival times $\mathbf{T} \in \mathbb{R}^n$ in n different points $\mathbf{x} = [x_1, x_2, x_3 ... x_n]$. This can be done manually, although various automatic approaches are also available [20]. Using (1)-(3), we can calculate the synthetic arrival times $\mathbf{t} \in \mathbb{R}^n$ for these $\mathbf{x} \in \mathbb{R}^n$ values subject to a given set of $\{x_0, d, R, \epsilon_r\}$. Given a set of real ($\mathbf{T}$) and synthetic ($\mathbf{t}$) measurements, we can express hyperbola fitting as an optimization problem to find the best $\{x_0, d, R, \epsilon_r\}$ that minimize the summation of the squared differences between the real and the synthetic arrival times, as described by

$$\underset{d, R, \epsilon_r \in \mathbb{R}}{\operatorname{argmin}} (\mathbf{t} - \mathbf{T}) \cdot (\mathbf{t} - \mathbf{T})^T \tag{4}$$

In order to avoid local minimal and potential optimization plateau [16], a hybrid approach is used here that combines particle swarm optimization (PSO) and convex optimization. PSO, which is a global optimizer, is initially employed, and the resulting $\{x_0, d, R, \epsilon_r\}$ are then used as initial points to the simplex method. The choice of PSO and simplex method is arbitrary, the optimization in (4) can be executed using any global optimizer (genetic algorithms, ant colony optimization etc.) combined with any convex method (non-linear least squares, gradient descent etc.).

III. Non-Uniqueness

In the following, we argue that conventional hyperbola fitting as described in (4) is not reliable for estimating R, for the level of accuracy needed in practical engineering applications such as utility detection and non-destructive testing. Through a series of numerical and laboratory experiments, we showcase that even a small amount of noise makes the problem ill-posed resulting to non-unique solutions. A minimum level of noise is expected even in clinical datasets due to A) errors in the digitisation of the hyperbola, B) non-homogeneous permittivity distributions, C) antenna positioning errors, D) surrounding clutter, E) antenna noise and F) errors in GPR time-zero correction. Consequently, apart from clinical numerical studies, where noise can be completely absent, conventional hyperbola fitting is not reliable for radius estimation.

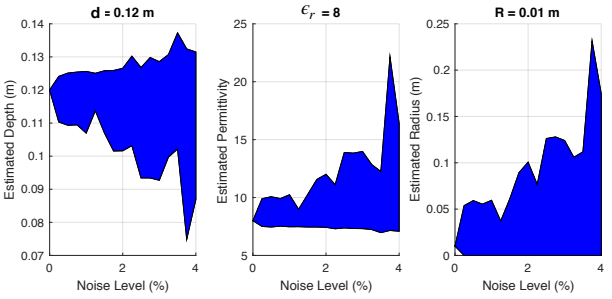

Fig. 4. Concrete inspection: 120 realisations of hyperbola fitting (4) for different sets of Gaussian noise in each execution. The real $\{d, R, \epsilon_r\}$ are shown on the titles of the subplots. The error for R can go up to 500% with less than 2% of noise level, falsely estimating the radius of the rebar anywhere from 0 up to 0.06 m. This range includes the whole spectrum of rebar sizes, adding no additional information to what is already expected.

For the first numerical case study, we consider a utility detection scenario, where a cylindrical pipe with $R = 0.1$ m is buried at $d = 1$ m in a homogeneous non-magnetic half-space with $\epsilon_r = 10$. The antenna is considered to be monostatic ($w = 0$), and the hyperbola is mapped at 2 meters symmetrically around x_0 with a 0.05 m step. The synthetic arrival times were calculated using (1) - (3). In the absence of noise, the optimization in (4), using PSO coupled with the simplex method, always converges to the correct results. This gives the false impression that hyperbola fitting can be used to accurately estimate the radius of cylindrical targets as discussed in [16]. Nonetheless, if the arrival times are corrupted with Gaussian noise, the problem becomes ill-posed and the solution to (4) is no longer unique. Executing the optimization in (4) 120 times, we get 120 different sets of $\{d, R, \epsilon_r\}$ that equally satisfy the noisy data. The uncertainty of the results with respect to the level of noise is shown in Fig. 2. The non-uniqueness of the problem is more clearly showcased in Fig. 3 where three different hyperbolas with different $\{d, R, \epsilon_r\}$ are plotted and are almost identical. The first one (solid line) corresponds to $d = 1$ m, $R = 0.1$ m, $\epsilon_r = 10$, the second one (circles) to $d = 0.97$ m, $R = 0.2$ m, $\epsilon_r = 10.6$, and the third one (stars) to $d = 0.91$ m, $R = 0.4$ m, $\epsilon_r = 12.1$. From Fig. 2 and 3 it is apparent, that with minimum level of noise both the permittivity and the depth of the target can be estimated within an accepted range of error. For the radius, the error can go as high as 500% falsely estimating the radius of the pipe anywhere from 0 up to 0.6 m. This range includes the whole spectrum of utility sizes, adding no additional information to what is already expected.

The second numerical study is based on a scenario typically encountered in non-destructive testing, and in particular in rebar detection and characterization. A cylindrical rebar with $R = 0.01$ m is buried at $d = 0.12$ m in a non-magnetic homogeneous half-space with $\epsilon_r = 8$. The antenna is considered monostatic ($w = 0$), and the hyperbola is mapped symmetrically 0.5 m around the target with a 0.01 m step. Similarly to the previous example, in the absence of noise, hyperbola fitting using (4) always converges to the correct solutions. Adding Gaussian noise to the arrival times, results to non-unique solutions as shown in Fig. 4. The non-uniqueness

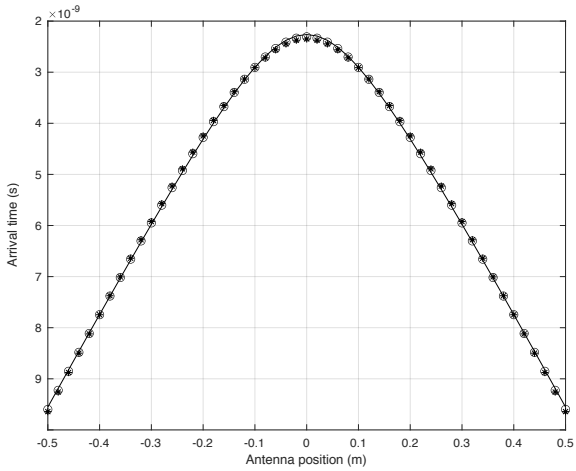

Fig. 5. Three almost identical hyperbolas with different $\{d, R, \epsilon_r\}$ are plotted together to illustrate the non-unique results of hyperbola fitting in the presence of noise. Solid line: $d = 0.12$ m, $R = 0.01$ m, $\epsilon_r = 8$; circles: $d = 0.118$ m, $R = 0.03$ m, $\epsilon_r = 8.5$; stars: $d = 0.116$ m, $R = 0.05$ m, $\epsilon_r = 9.1$.

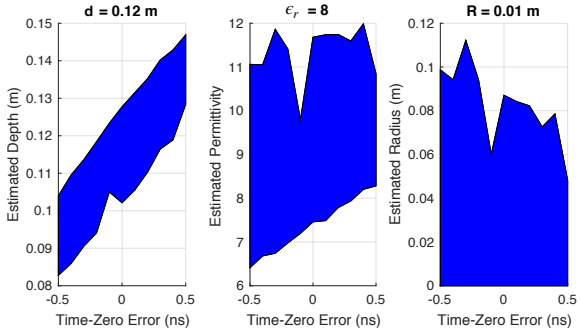

Fig. 6. The effect of time-zero error to the estimated $\{d, R, \epsilon_r\}$. The noise level is 1% for all the experiments. With blue colour is the range of $\{d, R, \epsilon_r\}$ that equally fits the arrival times. The real $\{d, R, \epsilon_r\}$ are shown on the titles of the subplots.

of the problem is more clearly shown in Fig. 5 where 3 different hyperbolas with different $\{d, R, \epsilon_r\}$ are plotted and are almost identical. The first one (solid line) corresponds to $d = 0.12$ m, $R = 0.01$ m, $\epsilon_r = 8$, the second one (circles) to $d = 0.118$ m, $R = 0.03$ m, $\epsilon_r = 8.5$, and the third one (stars) to $d = 0.116$ m, $R = 0.05$ m, $\epsilon_r = 9.1$. The range of radii that sufficiently fit the hyperbola is within the expected range of rebar sizes, adding no useful information to the survey.

Next we examine the effects of time-zero correction to the overall accuracy of hyperbola fitting. The previous case study ($R = 0.01$ m, $d = 0.12$ m, $\epsilon_r = 8$) is now further corrupted with artifacts from non-optimum time-zero correction, that manifests as an added constant to the arrival times. The results are shown in Fig. 6. Errors in time-zero mostly affect the estimated depth and radius, while they don't have major effects to the estimated permittivity.

IV. Experimental Verification

Two case studies are presented in this chapter to further support the premise that hyperbola fitting is not reliable for radius estimation. The first one is a coherent numerical

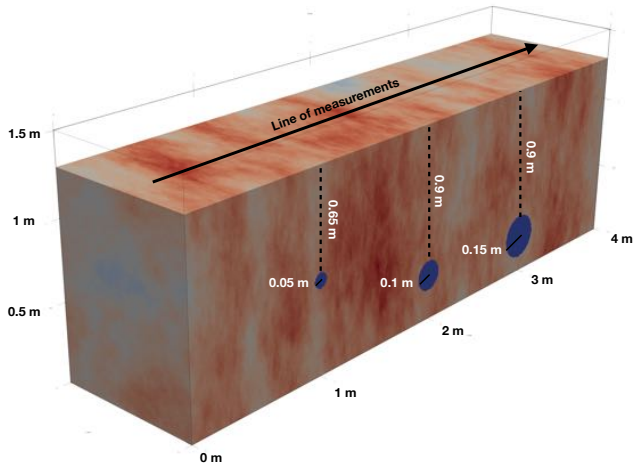

Fig. 7. The investigated numerical study. Three homogeneous low-dielectric ($\epsilon_r = 3$) pipes with different radii $R = [0.05, 0.1, 0.15]$ m, are buried in a stochastic medium with varying water fraction from 2-10% ($\epsilon_r \approx 4-9$). Red and light blue colours correspond to dry and saturated areas, respectively.

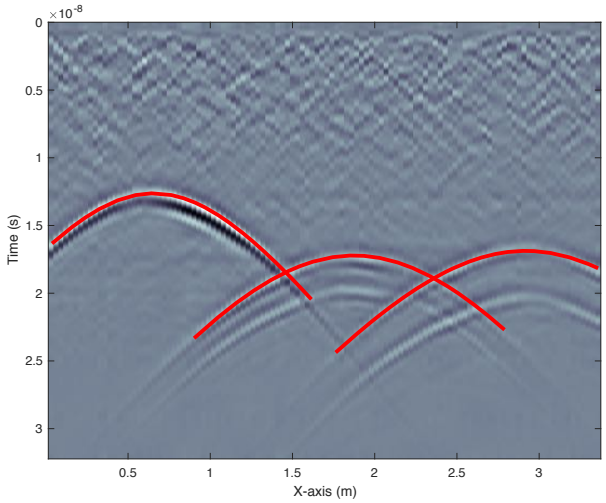

Fig. 8. The processed B-Scan from the model shown in Fig. 7. The fitted hyperbolas are not perfect due to the misshaped asymmetrical arrival times from the velocity variations. The resulting radii are $R = [0, 0.32, 0]$ m, with an average of 140 % error.

simulation of a typical scenario in utility detection, and the second is a laboratory experiment for concrete inspection.

A. Numerical Case Study

The investigated model is illustrated in Fig. 7. Three pipes with radii $R_1 = 0.05$ m, $R_2 = 0.1$ m and $R_3 = 0.15$ m are buried at $d_1 = 0.65$ m, $d_2 = 0.9$ m, $d_3 = 0.9$ m, respectively. All cylinders are uniform low dielectric targets with $\epsilon_r = 3$. They are buried in a realistic medium with stochastically varying dielectric properties ($\epsilon_r \approx 4 - 9$). In particular, the host medium has 50% sand and 50% clay, the bulk density of the soil is 2 gr/cm^3, the bulk density of the particles is 2.66 gr/cm^3 and the volumetric water fraction varies from $2 - 10$ %. The transmitter is a ground-coupled ideal Hertzian dipole with polarization parallel to the main axis of the pipes, and a 500 MHz central frequency. The offset between the transmitter and the receiver is $w = 0.04$ m, and measurements are taken every 0.03 m.

To simulate this model, we used gprMax [21], an open source electromagnetic solver that solves Maxwell's equations using a second order in both space and time finite-difference time-domain method. The spatial step of the model is $\Delta x = \Delta y = \Delta z = 0.009$ m, and the time step is set equal to 0.99 of the stability Courant limit. The dielectric properties of the soils are calculated based on the Dobson-Peplinski, the semi-empirical model available in gprMax [21].

The raw data were processed using time-zero correction, time-varying gain and singular value decomposition filter [18]. Furthermore, static components due to conductivity were fitted using a second order polynomial and subsequently removed from every trace. Fig. 8 shows the resulting processed BScan, and the fitted hyperbolas using (4). It can be seen that the fit is not perfect because the arrival times are misshaped and asymmetrical due to soil's heterogeneity. Hyperbola fitting manages to sufficiently approximate the permittivity $\epsilon_r = [6.2, 7.1, 5.1]$ and the cover depth of the targets $d = [0.76, 0.95, 1.08]$ m ($\approx 13\%$ error). As expected based on the results in the previous section, the radii of the pipes were not estimated correctly $R = [0, 0.32, 0]$ m, with an average of ≈ 140 % error making hyperbola fitting unreliable for radii estimation.

B. Laboratory Experiment

The investigated case study is shown in Fig. 9. The measurements were taken at the non-destructive testing laboratory at The University of Edinburgh. A mature concrete slab with six metallic rebars is scanned in order to showcase the ill-posed nature of conventional hyperbola fitting. The rebars have two different sizes $R = 0.00127$ m (#8 imperial size) and $R = 0.0079$ m (#6 imperial size). The measurements were taken perpendicular to the main axis of the rebars using the GSSI 2000MHz palm antenna. The measurement step is $\Delta x = 0.0078125$ m, and the offset between the transmitter and the receiver is $2w = 0.04$ m.

The processed BScan is shown in Fig. 10. Time-zero correction, zero-offset, background removal and time-gain are applied to the raw data. The hyperbolas for all six rebars are clearly visible in the processed BScan. Using hyperbola fitting to simultaneously estimate $\{d, R, \epsilon_r\}$ results to arbitrary values that can change picking slightly different arrival times. The unstable ill-posed nature of the problem is illustrated in Fig. 10 where the optimization in (4) is executed for each of the hyperbolas while constraining the radius to a specific size. The investigated radii are $R = [0, 0.015, 0.03, 0.045]$ m. For all the investigated R, hyperbola fitting manages to find a set of $\{d, \epsilon_r\}$ that sufficiently fits the measured hyperbolas. Depending on the assumed value of R, the estimated permittivities vary from $\epsilon \approx 7 - 11$ while the cover depths have a ± 1 cm accuracy.

From Fig. 10 it is apparent that conventional hyperbola fitting is unreliable for estimating the radii of rebars in concrete inspection. The non-unique nature of the problem makes it unstable regardless of the methodology chosen to interpret the measured hyperbola. The only way to overcome this is

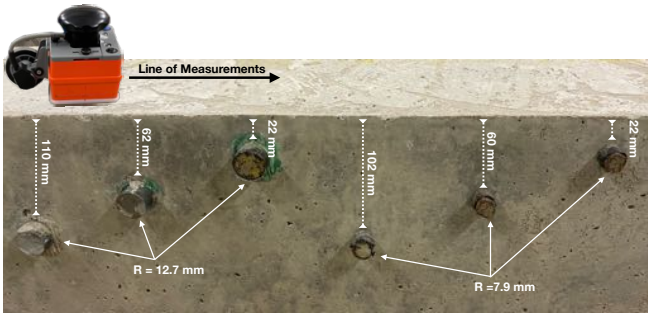

Fig. 9. Six rebars with different radii are embedded in a mature concrete slab. The rebars are metallic with #6 and #8 imperial size, arranged diagonally in two pairs of threes. The measurements are taken perpendicular to the main axis of the rebars using the commercial antenna GSSI 2000 MHz.

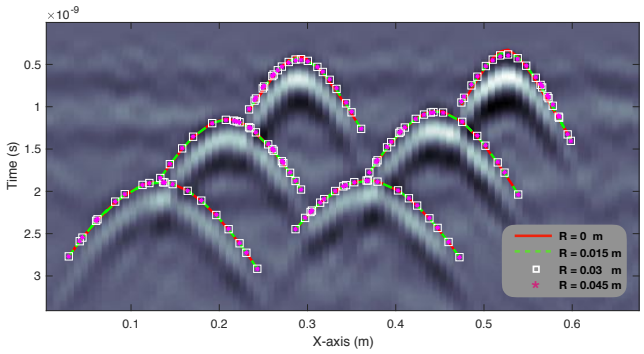

Fig. 10. The processed BScan for the case study shown in Fig. 9. Hyperbola fitting is used to interpret the measured arrival times for each target. The optimization in (4) is executed four times for each of the hyperbolas while constraining the radius to be equal with $R = [0, 0.015, 0.03, 0.045]$ m. The non-unique nature of the problem is apparent from the fact that there is a set of $\{d, \epsilon_r\}$ for all the investigated radii that sufficiently fits the measured arrival times.

to have clinically noise-less data-sets (which is unrealistic), or constrain the problem using independent methodologies for estimating either the permittivity of the medium or the cover depth of the target.

V. Conclusions

Through a series of numerical and laboratory experiments we have shown that conventional hyperbola fitting is not reliable for estimating the radii of cylindrical targets at the level of accuracy needed for practical utility detection and concrete inspection. Hyperbola fitting, can sufficiently estimate the permittivity and depth of the targets, but regarding radius, errors up to 500% can occur in the presence of minimum level of noise. It is evident that unless perfectly noiseless data are available the current hyperbola fitting approaches are not able to reliably retrieve useful information about the radius of a target as it has been claimed in the literature.

Acknowledgements

This work was supported by the The Royal Society International Exchanges Cost Share 2020, and the National Natural Science Foundation of China (Grant No. 42111530126).

References

[1] D. J. Daniels, *Ground Penetrating Radar*. American Cancer Society, 2005.

[2] L. Pajewski, A. Benedetto, X. Derobert, A. Giannopoulos, A. Loizos, G. Manacorda, M. Marciniak, C. Plati, G. Schettini, and I. Trinks, "Applications of ground penetrating radar in civil engineering — cost action tu1208," in *2013 7th International Workshop on Advanced Ground Penetrating Radar*, 2013, pp. 1–6.

[3] Q. Lu, C. Liu, Y. Wang, S. Liu, Z. Zeng, X. Feng, and S. She, "Ground penetrating radar applications in mapping underground utilities," in *2018 17th International Conference on Ground Penetrating Radar (GPR)*, 2018, pp. 1–4.

[4] I. Giannakis, A. Giannopoulos, and C. Warren, "A machine learning scheme for estimating the diameter of reinforcing bars using ground penetrating radar," *IEEE Geoscience and Remote Sensing Letters*, vol. 18, no. 3, pp. 461–465, 2021.

[5] N. J. Cassidy, "Chapter 5 - ground penetrating radar data processing, modelling and analysis," in *Ground Penetrating Radar Theory and Applications*, H. M. Jol, Ed. Amsterdam: Elsevier, 2009, pp. 141–176.

[6] C. W. Chang, C. H. Lin, and H. S. Lien, "Measurement radius of reinforcing steel bar in concrete using digital image gpr," *Construction and Building Materials*, vol. 23, no. 2, pp. 1057–1063, 2009.

[7] S. Jazayeri, A. Klotzsche, and S. Kruse, "Improving estimates of buried pipe diameter and infilling material from ground-penetrating radar profiles with full-waveform inversion," *Geophysics*, vol. 83, no. 4, pp. H27–H41, 2018.

[8] A. V. Ristic, D. Petrovacki, and M. Govedarica, "A new method to simultaneously estimate the radius of a cylindrical object and the wave propagation velocity from gpr data," *Computers Geosciences*, vol. 35, no. 8, pp. 1620–1630, 2009.

[9] R. Jaufer, S. Todkar, A. Ihamouten, Y. Goyat, D. Guilbert, A. Caucheteux, V. Baltazart, C. Heinkele, and X. Dérobert, "Ray-based method vs. svm for the inversion of embedded cylindrical pipe's parameters from gpr data: Numerical comparative study," *SEG Global Meeting Abstracts*, vol. 209, pp. 356–359, 2020.

[10] R. Jaufer, A. Ihamouten, S. S. Todkar, F. Bosc, Y. Goyat, and X. Dérobert, "Use of deep lerning on gpr data for parameter inversion of buried cylindrical pipes," vol. 2021, no. 1, pp. 1–5, 2021.

[11] N. Muniappan, E. P. Rao, A. V. Hebsur, and G. Venkatachalam, "Radius estimation of buried cylindrical objects using gpr — a case study," in *2012 14th International Conference on Ground Penetrating Radar (GPR)*, 2012, pp. 789–794.

[12] A. Dolgiy, A. Dolgiy, and V. Zolotarev, "Gpr estimation for diameter of buried pipes," 2005.

[13] L. Mertens, R. Persico, L. Matera, and S. Lambot, "Automated detection of reflection hyperbolas in complex gpr images with no ¡italic¿a priori¡/italic¿ knowledge on the medium," *IEEE Transactions on Geoscience and Remote Sensing*, vol. 54, no. 1, pp. 580–596, 2016.

[14] A. Simi, S. Bracciali, and G. Manacorda, "Hough transform based automatic pipe detection for array gpr: Algorithm development and on-site tests," in *2008 IEEE Radar Conference*, 2008, pp. 1–6.

[15] H. Chen and A. G. Cohn, "Probabilistic robust hyperbola mixture model for interpreting ground penetrating radar data," in *The 2010 International Joint Conference on Neural Networks (IJCNN)*, 2010, pp. 1–8.

[16] R. M. Jaufer, A. Ihamouten, Y. Goyat, S. S. Todkar, D. Guilbert, A. Assaf, and X. Dérobert, "A preliminary numerical study to compare the physical method and machine learning methods applied to gpr data for underground utility network characterization," *Remote Sensing*, vol. 14, no. 4, 2022.

[17] W. Lei, F. Hou, J. Xi, Q. Tan, M. Xu, X. Jiang, G. Liu, and Q. Gu, "Automatic hyperbola detection and fitting in gpr b-scan image," *Automation in Construction*, vol. 106, p. 102839, 2019.

[18] I. Giannakis, F. Tosti, L. Lantini, and A. M. Alani, "Health monitoring of tree trunks using ground penetrating radar," *IEEE Transactions on Geoscience and Remote Sensing*, vol. 57, no. 10, pp. 8317–8326, 2019.

[19] R. Wang, Y. Su, C. Ding, S. Dai, C. Liu, Z. Zhang, T. Hong, Q. Zhang, and C. Li, "A novel approach for permittivity estimation of lunar regolith using the lunar penetrating radar onboard chang'e-4 rover," *Remote Sensing*, vol. 13, no. 18, 2021.

[20] Q. Dou, L. Wei, D. R. Magee, and A. G. Cohn, "Real-time hyperbola recognition and fitting in gpr data," *IEEE Transactions on Geoscience and Remote Sensing*, vol. 55, no. 1, pp. 51–62, 2017.

[21] C. Warren, A. Giannopoulos, and I. Giannakis, "gprmax: Open source software to simulate electromagnetic wave propagation for ground penetrating radar," *Computer Physics Communications*, vol. 209, pp. 163 – 170, 2016.